Fourier Transform Ion Cyclotron Resonance Mass Spectrometry: Fundamental Concepts

Peter B. O'Connor

Critical Literature:

Qi, Y.; O'Connor, P. B., Data processing in Fourier transform ion cyclotron resonance mass spectrometry. *Mass Spectrometry Reviews* ***2014,*** *33, 333-352****.***

Amster, I. J. Fourier Transform Mass Spectrometry *J. Mass Spectrom.* **1996**, *31*, 1325-1337.

Zhang, L. K.; Rempel, D.; Pramanik, B. N.; Gross, M. L. Accurate mass measurements by Fourier transform mass spectrometry *Mass Spectrom. Rev.* **2005**, *24*, 286-309.

Marshall, A. G.; Hendrickson, C. L.; Jackson, G. S. Fourier Transform Ion Cyclotron Resonance Mass Spectrometry - A Primer *Mass Spectrom. Rev.* **1998**, *17*, 1-35.

Special thanks to:

Mike Easterling (Bruker) and Jon Amster (Univ. Georgia) for slides.

FTICR-MS YouTube Video

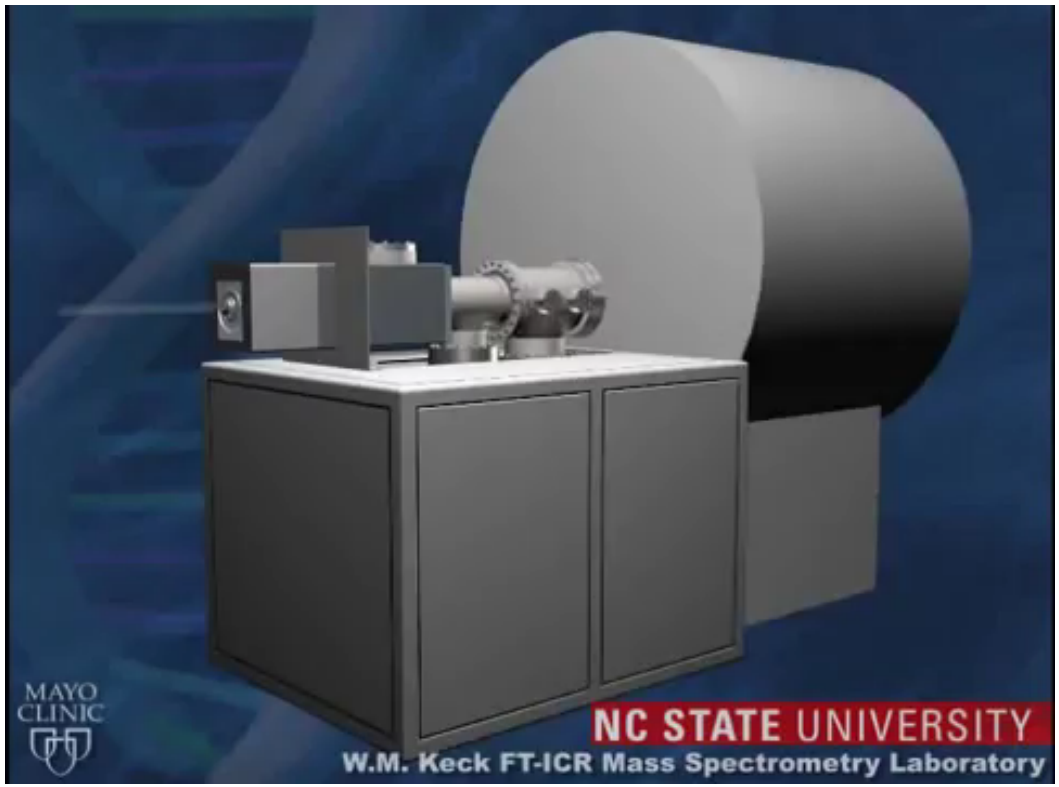

David Muddiman's FTICR-MS Youtube Video:
https://www.youtube.com/watch?v=7EHngA4S3Ws

Outline

- FTICR instruments
- Pulse sequences
- Ion motion
- Equations and calibration
- Excite/detect
- Resolving power
- Space Charge
- 2-Dimensional mass spectrometry

FTICR MS Instruments in 2005

Thermo

Varian, Inc

Bruker Daltonics

solarix

BRUKER

Next-Generation FTMS

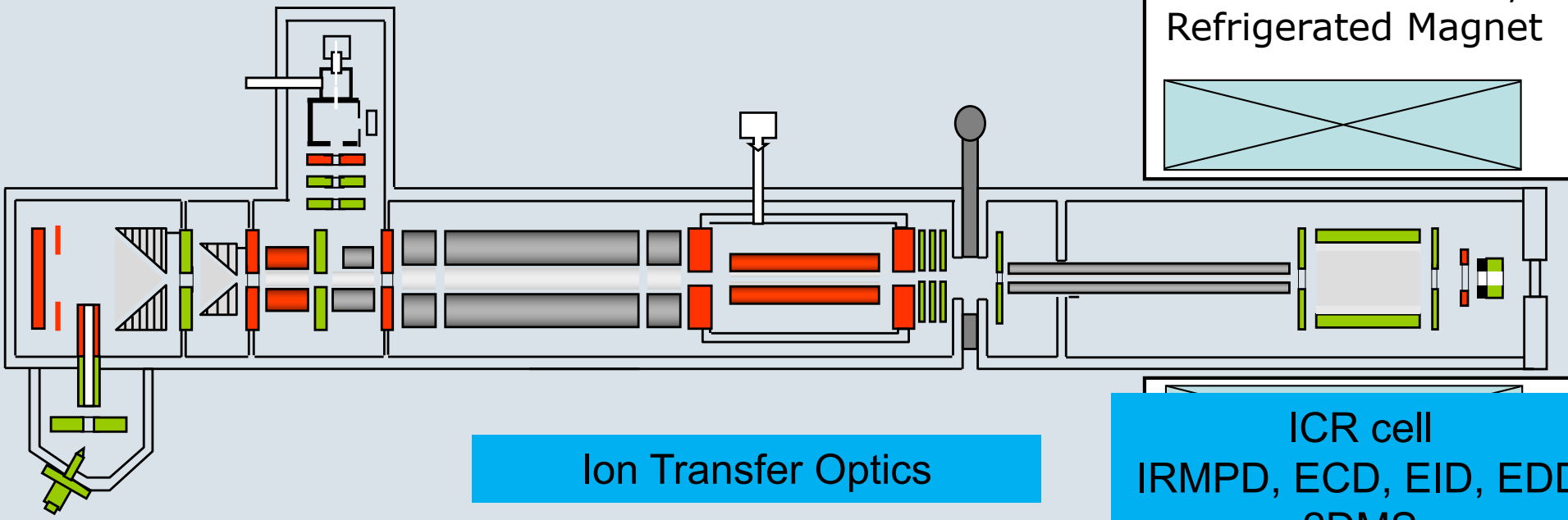

Bruker's scimaX FTICR mass spectrometer with a conductively cooled magnet.

Released June 2018

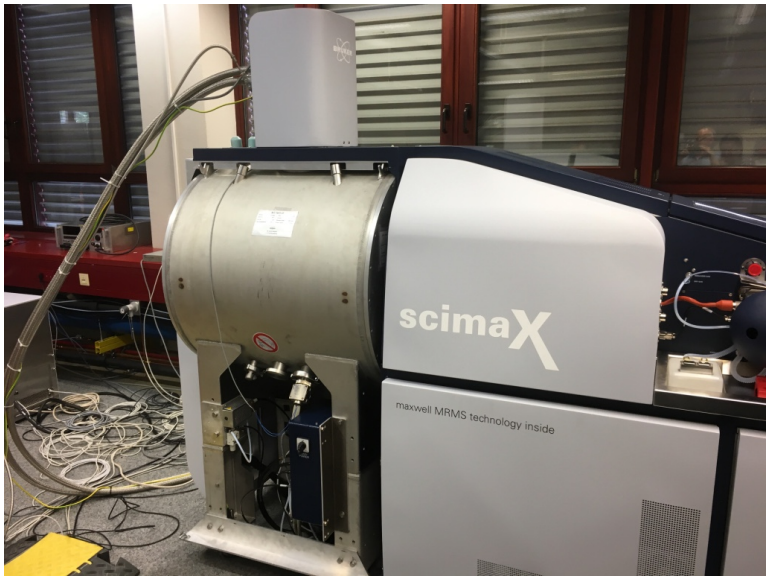

Our experiments get easier

at higher magnetic fields

Linear increases

Highest Non-Coalesced Mass
Mass Resolving Power
Scan Speed (LC/MS)

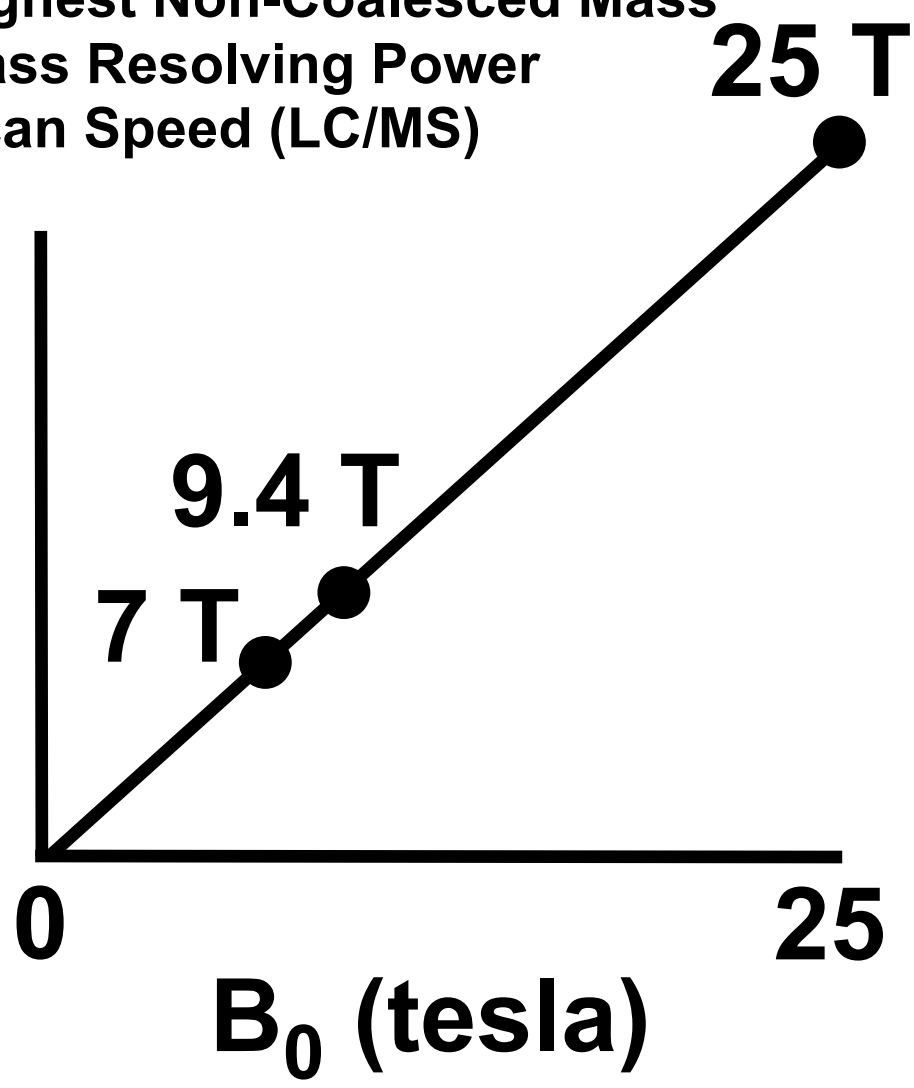

Increase as B^2

Ion Energy
Number of Ions
Upper Mass Limit
Ion Trapping Time

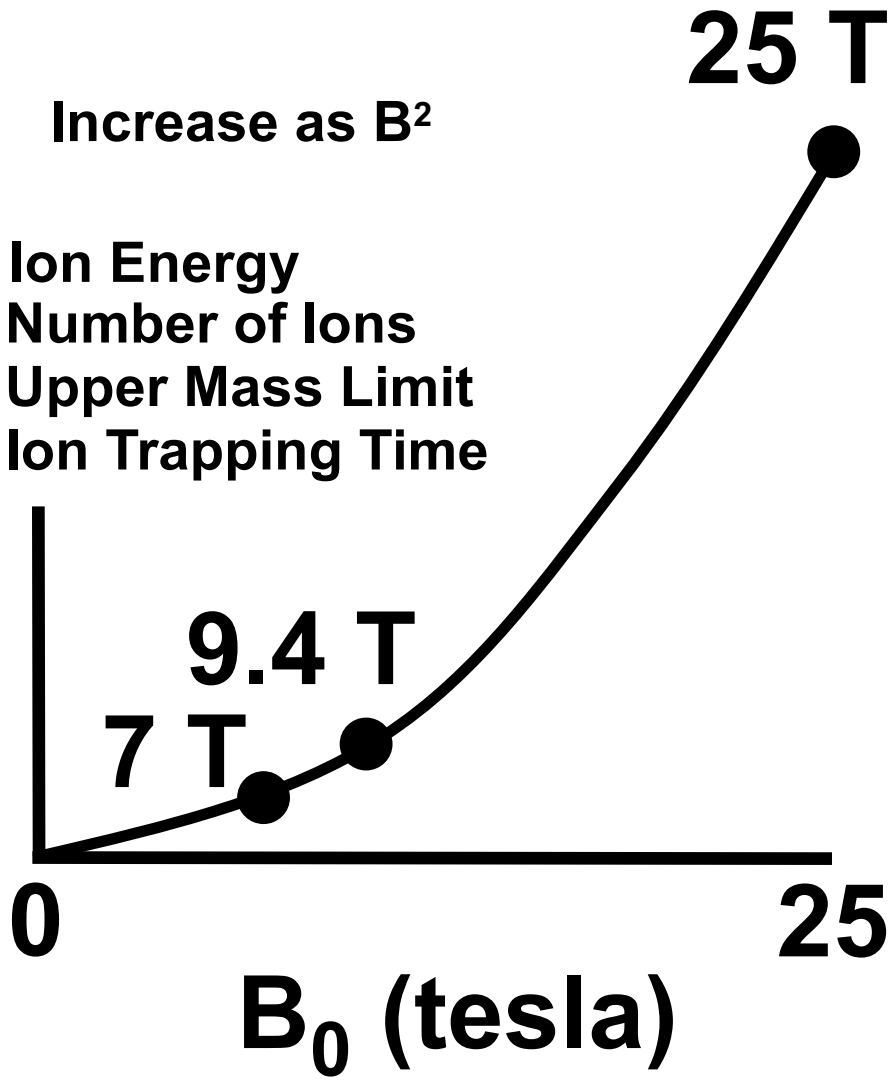

A.G. Marshall, C.L. Hendrickson, G.S. Jackson, *Mass Spectrom. Rev.* (1998) 17, 1-35

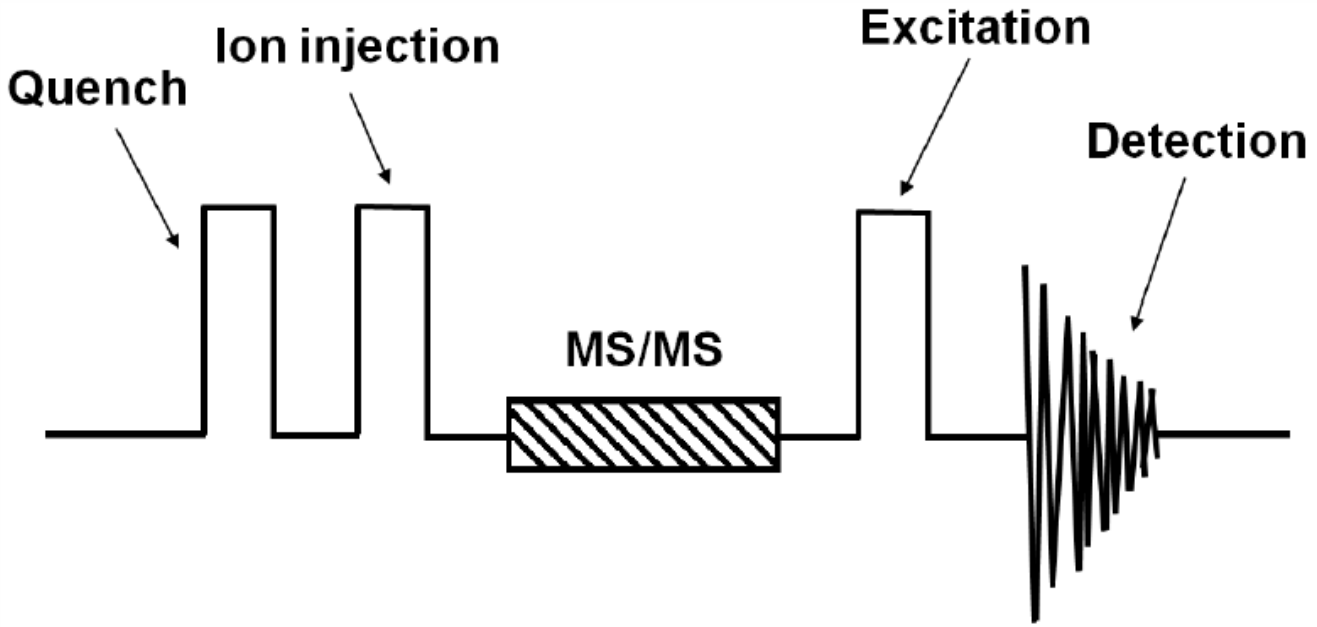

Figure 3. A simple experimental pulse program of FT-ICR

Qi, Y.; O'Connor, P. B., Data processing in Fourier transform ion cyclotron resonance mass spectrometry. *Mass Spectrometry Reviews* ***2014, 33 (5), 333-352.***

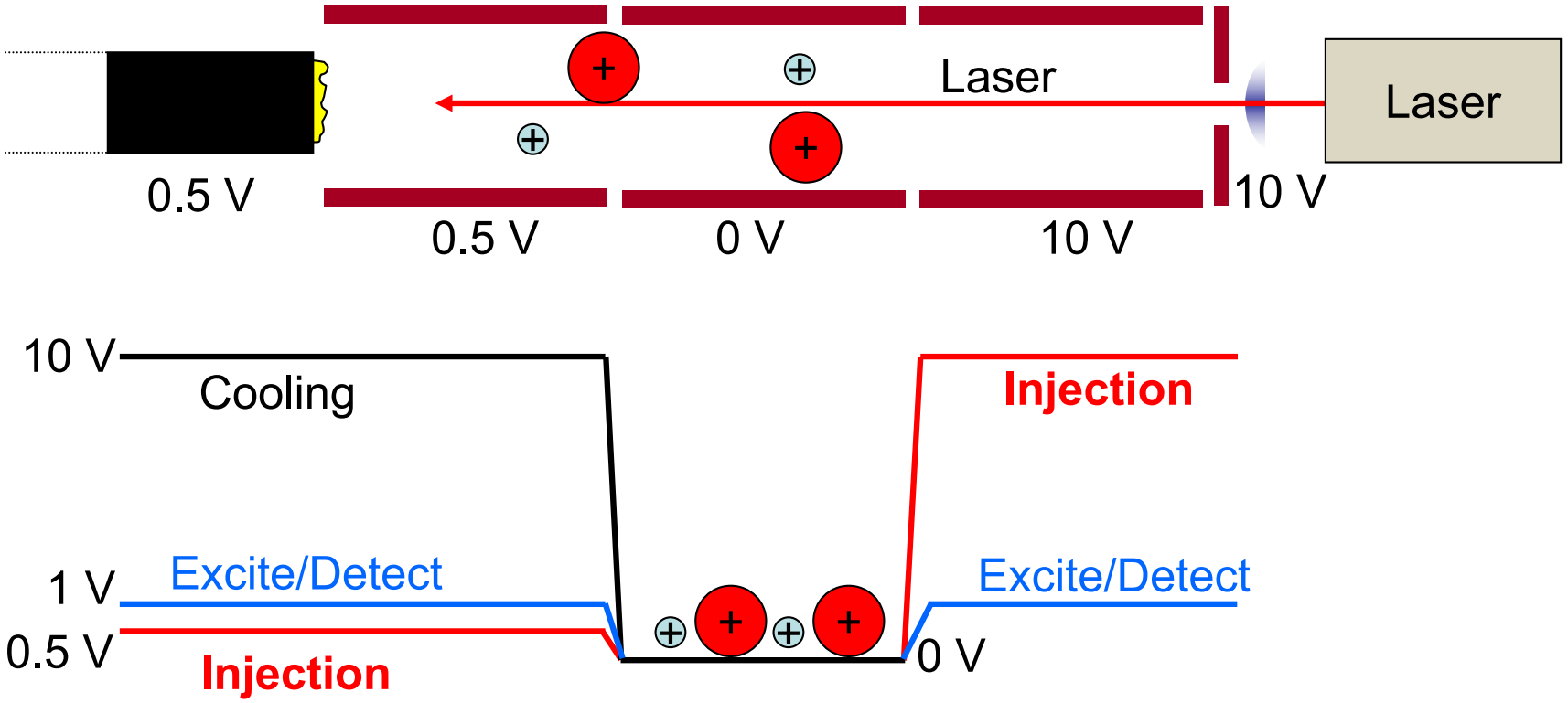

Figure 6. In-cell MALDI FTMS.

Outline

- FTICR instruments
- Pulse sequences
- Ion motion
- Equations and calibration
- Excite/detect
- Resolving power
- Space Charge
- 2-Dimensional mass spectrometry

Initialize Trap Voltages

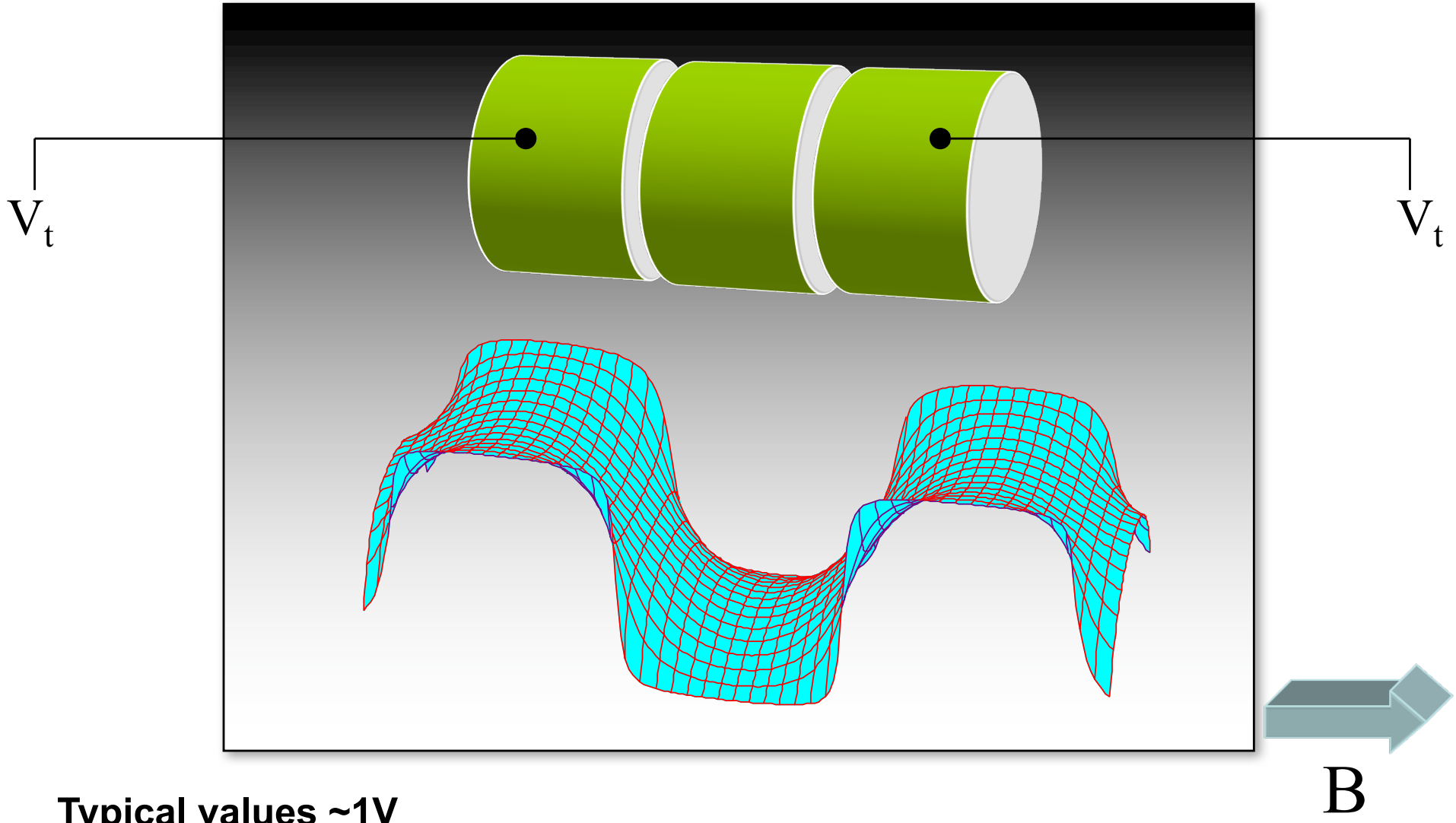

Typical values ~1V

Ion Motion in a Magnetic Field

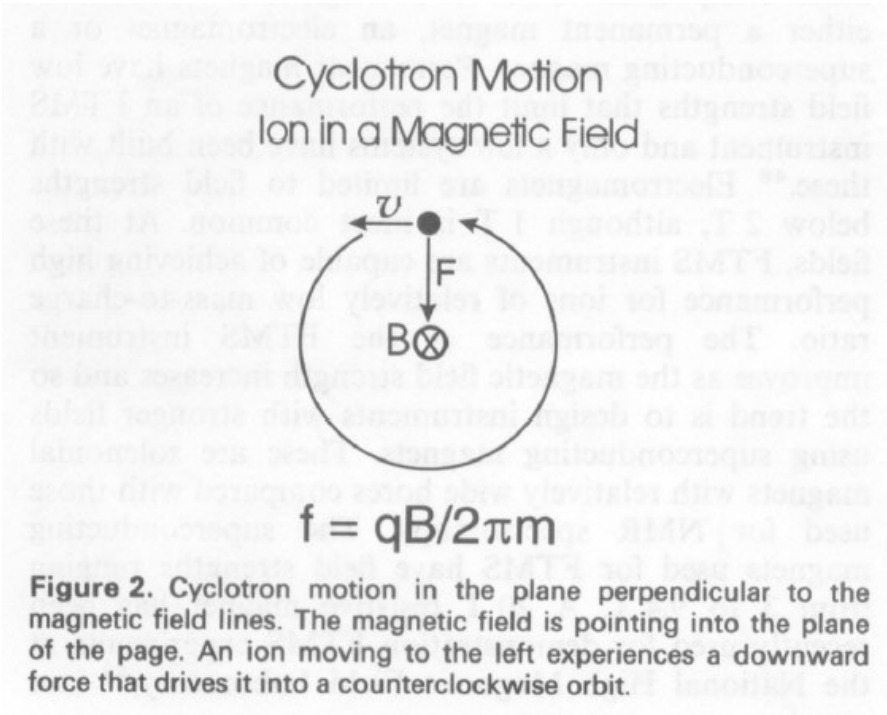

Figure 2. Cyclotron motion in the plane perpendicular to the magnetic field lines. The magnetic field is pointing into the plane of the page. An ion moving to the left experiences a downward force that drives it into a counterclockwise orbit.

One force equation

$$\mathbf{F} = q\mathbf{E} + q(\mathbf{v} \otimes \mathbf{B})$$

One equation of motion

$$\frac{d\mathbf{v}}{dt} = \left(\frac{q}{m}\right)(\mathbf{E} + \mathbf{v} \times \mathbf{B}) - \xi\mathbf{v}$$

Three cartesian equations of motion

$$\frac{d^2x}{dt^2} = \frac{q}{m}E_x + \frac{q}{m}\frac{dy}{dt}B_z - \xi\frac{dx}{dt}$$

$$\frac{d^2y}{dt^2} = \frac{q}{m}E_y + \frac{q}{m}\frac{dx}{dt}B_z - \xi\frac{dy}{dt}$$

$$\frac{d^2z}{dt^2} = \frac{q}{m}E_z - \xi\frac{dz}{dt}$$

Z- Axial Motion

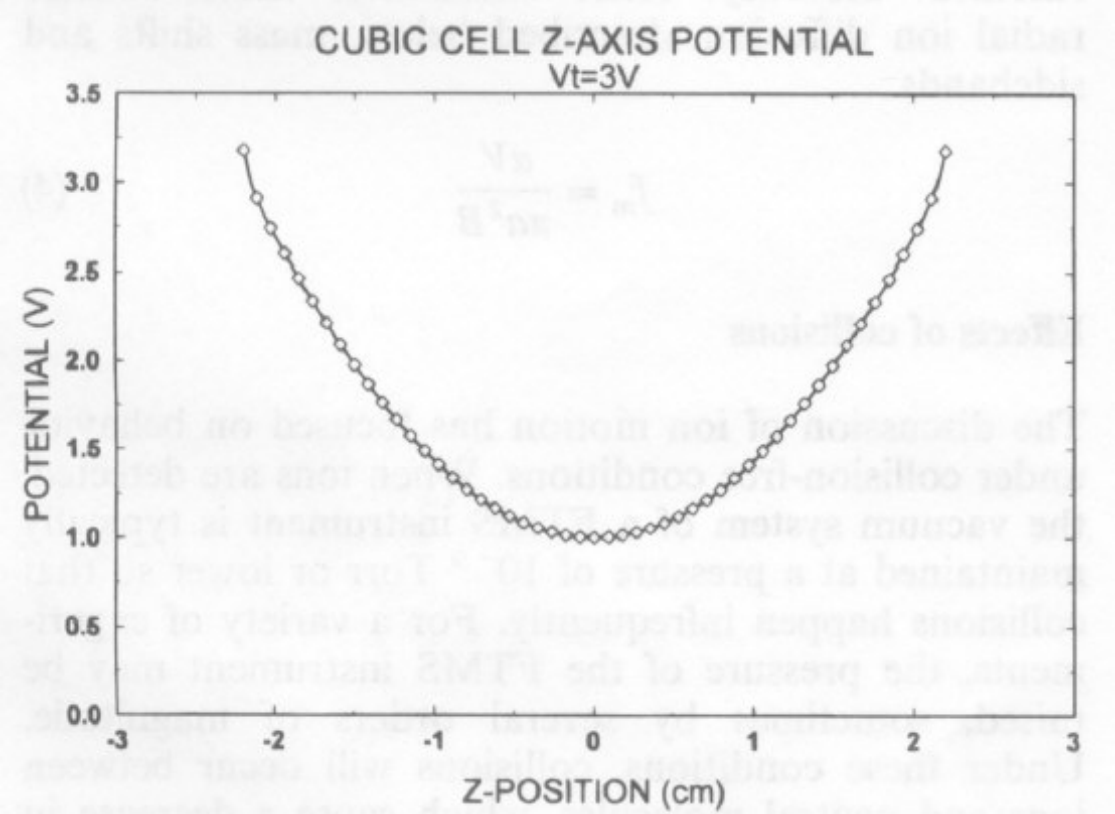

Figure 3. A plot of the electric potential due to the trapping voltage in a cubic cell along the principal axis that lies parallel to the magnetic field, the z-axis. The potential at the center of the cell is one-third of the trapping voltage.

Standard damped oscillator equation

$$\frac{d^2z}{dt^2} = \frac{q}{m}E_z - \xi\frac{dz}{dt}$$

if ξ=0 (good assumption) this is a standard parabolic oscillator solution:

$$\omega_z = \frac{2}{a}\sqrt{\frac{\alpha q V_{eff}}{m}}$$

a = cell plate spacing, α = geometry constant (0.273 for cubic cell)

Cyclotron Motion

$$\frac{d^2x}{dt^2} + \xi\frac{dx}{dt} - \frac{q}{m}\frac{V_{eff}x}{a} - \omega_c\frac{dy}{dt} = 0$$

$$\frac{d^2y}{dt^2} + \xi\frac{dy}{dt} - \frac{q}{m}\frac{V_{eff}y}{a} - \omega_c\frac{dx}{dt} = 0$$

if ξ=0 (somewhat good assumption) this equation can be solved by the quadratic equation:

$$\omega_{obsd}^2 - \omega_c\omega_{obsd} + \frac{V_{eff}}{a}\frac{q}{m} = 0$$

$$\boldsymbol{\omega_c = \frac{qB}{m}}$$

$$\omega_{obsd} = \frac{\omega_c \pm \sqrt{\omega_c^2 - 4(\frac{V_{eff}q}{am})}}{2}$$

Calibration Equations

Zhang, L. K.; Rempel, D.; Pramanik, B. N.; Gross, M. L. Accurate mass measurements by Fourier transform mass spectrometry *Mass Spectrom. Rev.* **2005**, *24*, 286-309.

TABLE 1. Proposed calibration procedures

$f = \frac{a}{m}$	basic law of ions in a B field
$f^2 = \frac{a}{m^2} + \frac{b}{m}$	(Beauchamp-Armstrong et al., 1969)
$f^2 = \frac{a}{m^2} + \frac{b}{m} + c$	(Ledford et al., 1980)
$f_{sideband} = \frac{a}{m}$	(Allemann et al., 1981)
$f = \frac{a}{m} + c$	(Francl et al., 1983)
$\left(\frac{M}{Z}\right) = \frac{a}{f_{obsd}} + \frac{b}{f_{obsd}^2}$	(Ledford et al., 1984b)
$f_{estimated} = f_{measured} + c(I_{calibrant} - I_{analyte})$	
$\frac{m}{z} = \frac{A}{f_{estimated}} + \frac{B}{f_{estimated}^2} + \frac{C}{f_{estimated}^3}$	(Easterling et al., 1999)
$M = (\frac{kB}{f_n + \Delta f})n - n(M_c)$	(Bruce et al., 2000)
$\left(\frac{M}{Z}\right)_i = \frac{a}{f_{obsd}} + \frac{b}{f_{obsd}^2} + \frac{CI_i}{f_{obsd}^2}$	(Masselon et al., 2002)
$\frac{m}{z} = \frac{A}{v} + \frac{B}{v^2} + \frac{C}{v^3} + \frac{BC}{Av^4}$	(Wang et al., 1988)

Francl, T. J.; *et al*, *Int. J. Mass Spec.* ***1983, 54, 189-199.***
Ledford, E. B., Jr.; Rempel, D. L.; Gross, M. L., *Anal. Chem.* ***1984, 56, 2744-2748.***

Magnetron motion

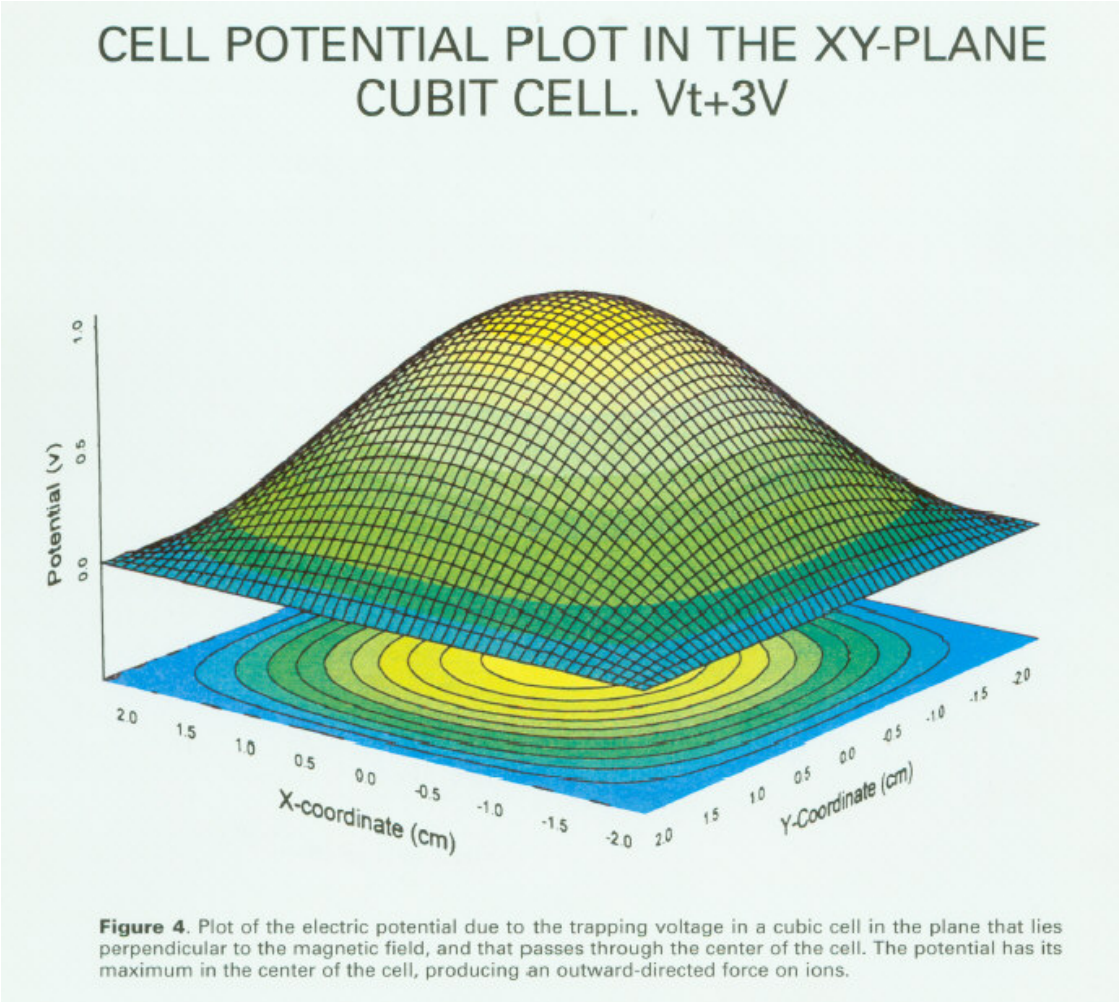

Figure 4. Plot of the electric potential due to the trapping voltage in a cubic cell in the plane that lies perpendicular to the magnetic field, and that passes through the center of the cell. The potential has its maximum in the center of the cell, producing an outward-directed force on ions.

$$f_m = \frac{\alpha V}{\pi a^2 B}$$

High Vacuum

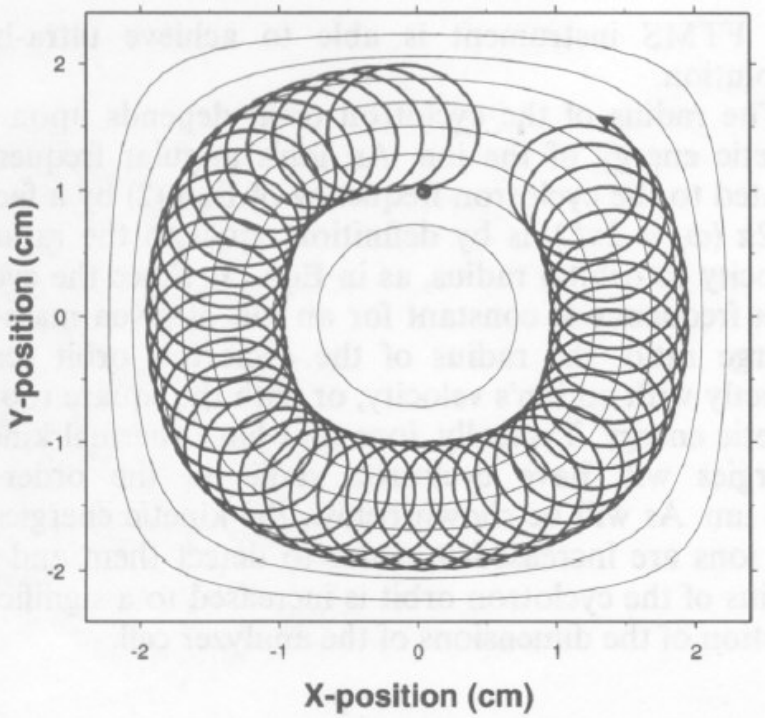

Figure 5. An ion trajectory that shows both cyclotron and mag netron motion plotted on the isopotential contours that result fror the trapping voltage. The trajectory is for an ion of *m/q* 500 wit 2 eV of kinetic energy in the xy-plane in a 4.4 cm cubic cell with 3 V trapping potential at 1 T magnetic field strength. Magnetro motion causes the guiding center of the cyclotron motion t precess around the cell along one isopotential contour. The ion' trajectory begins at the coordinates (0, 1) and ends at (1.2, 1.5). This trajectory shows ion motion in the absence of a collision gas.

High Pressure

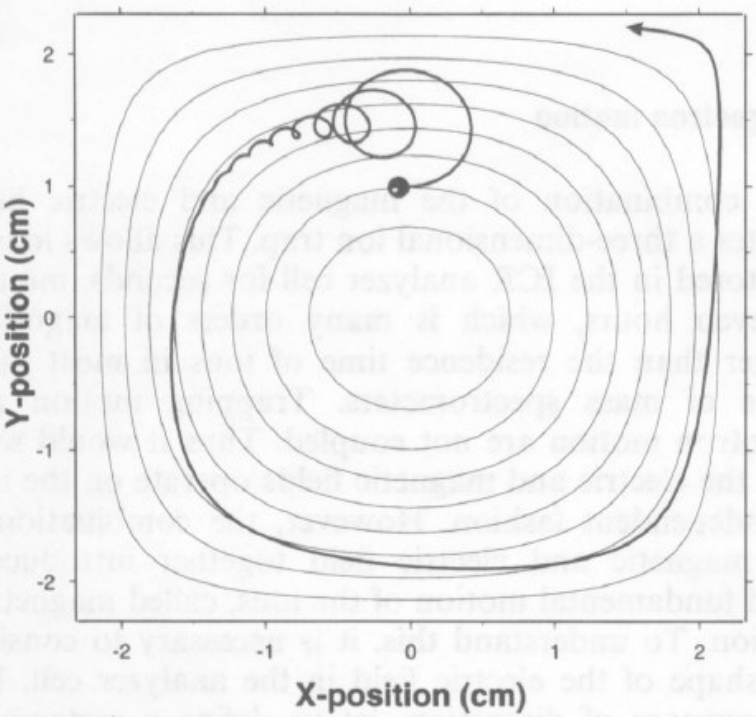

Figure 6. Effect of a collision gas upon ion motion. The initial conditions for the ion are the same as in Fig. 5, but a collision gas is present at a pressure of 0.01 Torr. Cyclotron motion is seen to damp quickly with a collapse of the cyclotron orbit, while the magnetron radius increases as motion in this coordinate slowly damps.

What assumptions have we made?

- Magnetic field is homogeneous
- Electric field is homogeneous
  - no space charge
  - cell plates are clean
  - ions oscillate independently
  - electric circuits have no resistance
- No background gas

Outline

- FTICR instruments
- Pulse sequences
- Ion motion
- Equations and calibration
- Excite/detect
- Resolving power
- Space Charge
- 2-Dimensional mass spectrometry

ICR Cell

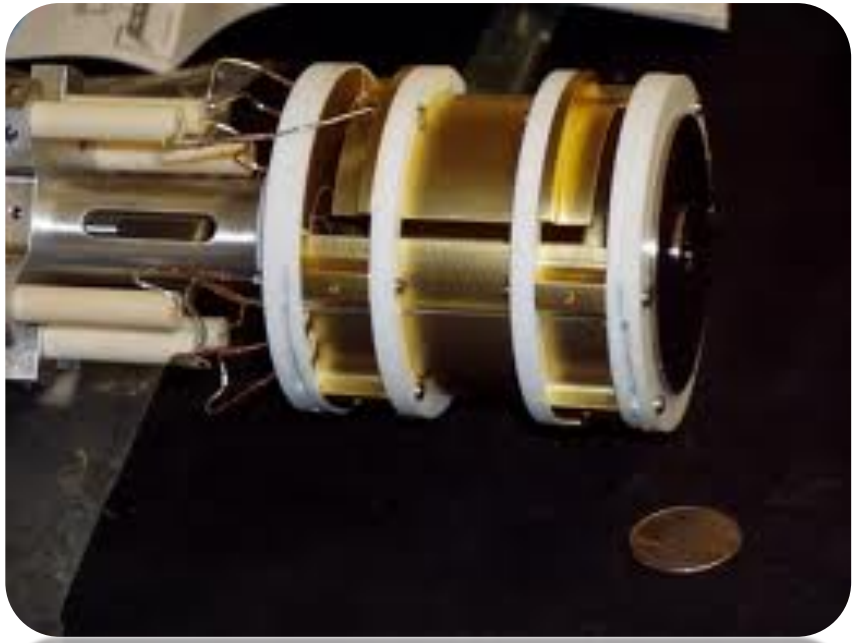

Caravatti, P.; Allemann, M., RF Shim by Trap Segmentation. *Org. Mass Spectrom.* ***1991, 26, 514-518.***

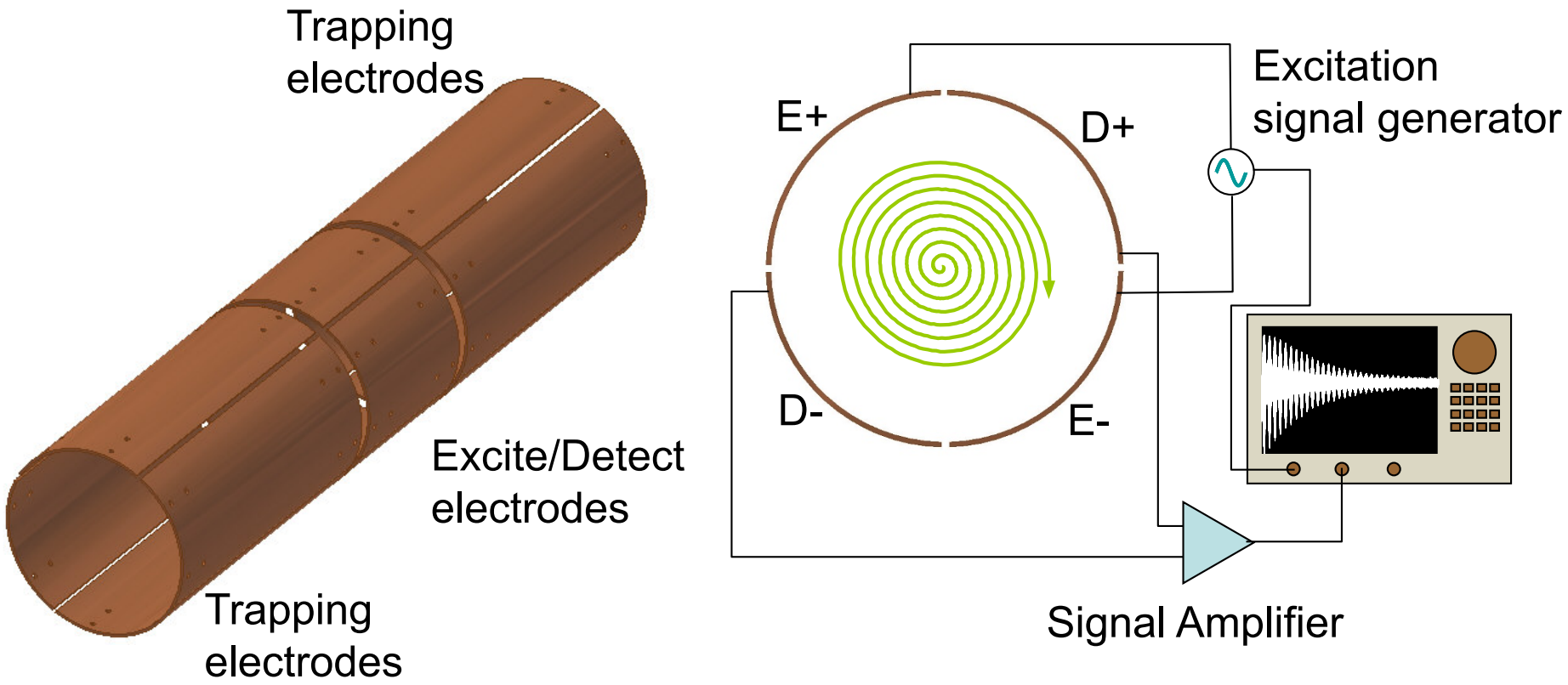

A. Typical open cylindrical cell

B. Typical Excite/Detect geometry

Figure 5. The principle of FT-ICR-MS.

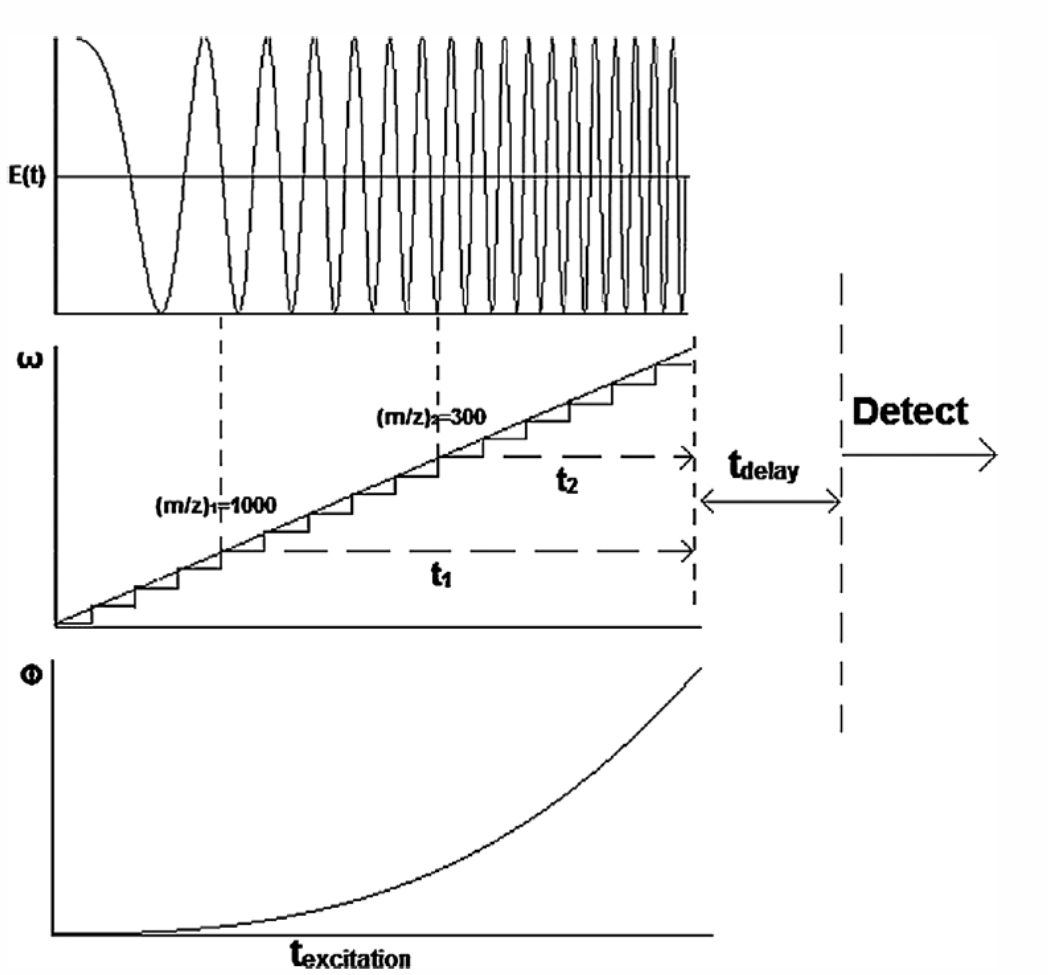

FIGURE 4. Top: Time-domain profiles of the RF chirp for ion excitation. Middle: Frequency for a linear polarized (upper line) or stepwise (lower line) frequency sweep. Bottom: Quadratic phase accumulation for the stepwise frequency sweep. Reprinted from Qi et al. (2011a), with permission from Springer, copyright 2011.

FTMS Ion Detection Method

- Image Current Detection

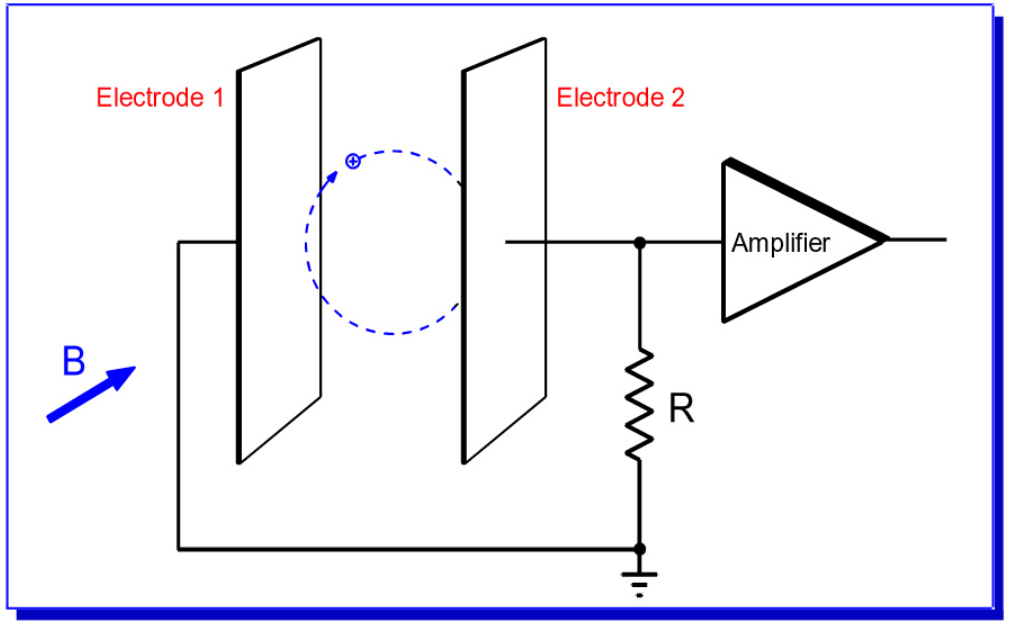

Shaw, J. B.; Gorshkov, M. V.; Wu, Q.; Pasa-Tolic, L., high Speed Intact Protein Characterization Using 4x Frequency Multiplication, Ion Trap Harmonization, and 21 Tesla FTICR-MS. *Anal Chem* ***2018.***
DOI: 10.1021/acs.analchem.7b04606

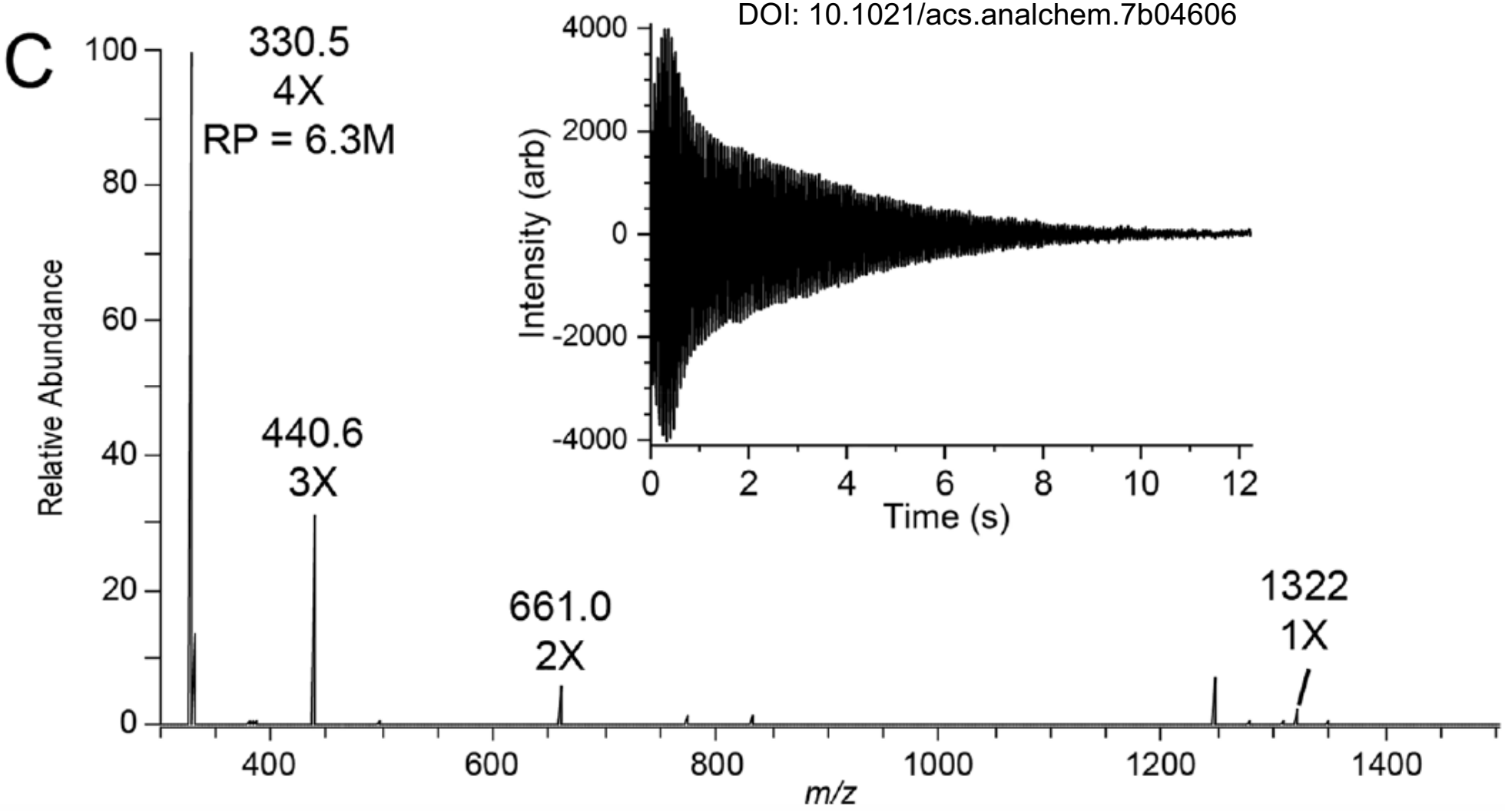

Outline

- FTICR instruments
- Pulse sequences
- Ion motion
- Equations and calibration
- Excite/detect
- Resolving power
- Space Charge
- 2-Dimensional mass spectrometry

Resolving Power in FTMS

Effect of Transient Length

There is a simple equation that relates the resolving power to the cyclotron frequency and the observation time of the signal.

Fourier Limit

$$\frac{M}{\Delta M_{1/2}} = RP_{MAX} = \frac{ft}{2}$$

f = frequency (Hz)
t = observation time

For example, if an ion with cyclotron frequency 500,000 Hz is detected for 1.0s, the resolving power is

$$\frac{M}{\Delta M_{1/2}} = 250,000$$

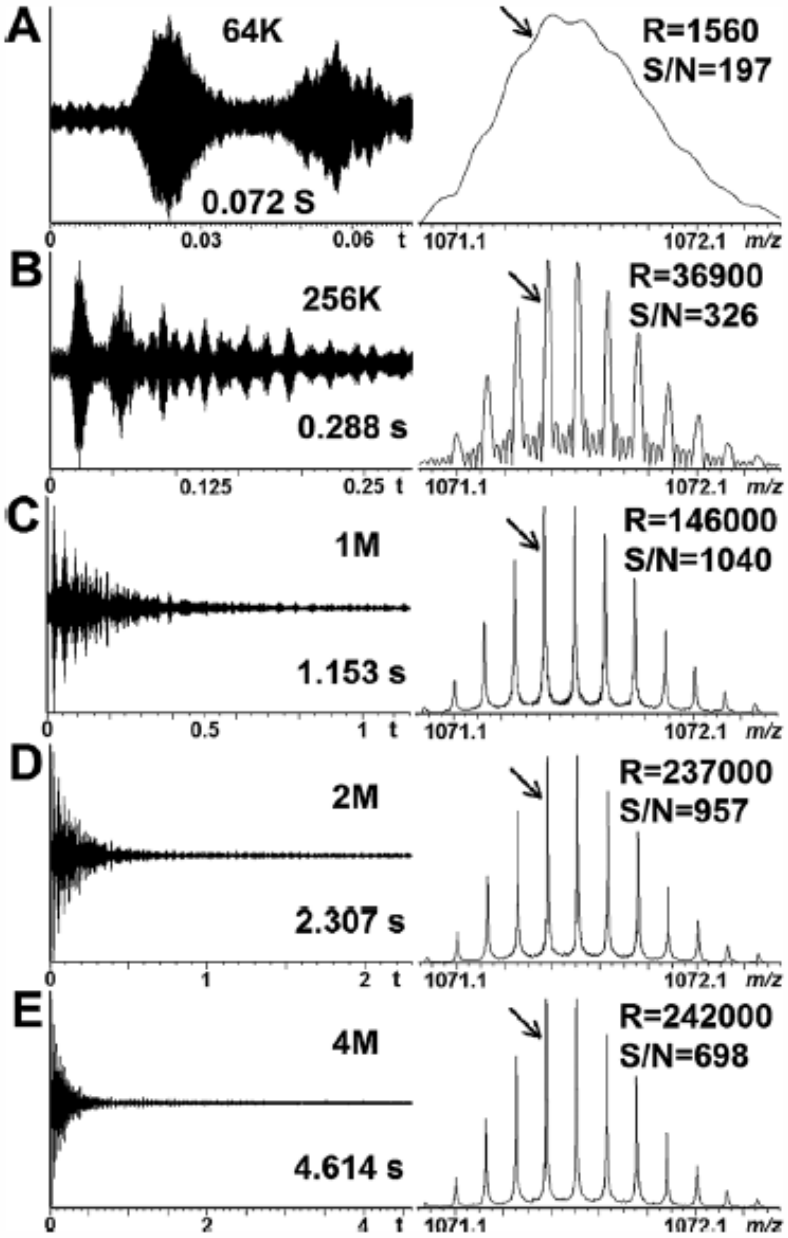

FIGURE 5. A ubiquitin data set (no apodization, one zero fill) demonstrates the transient duration (left), and its effect on the 8^+ isotopic peaks (right), the value of *R* and S/N are measured for the labeled peak in each spectrum.

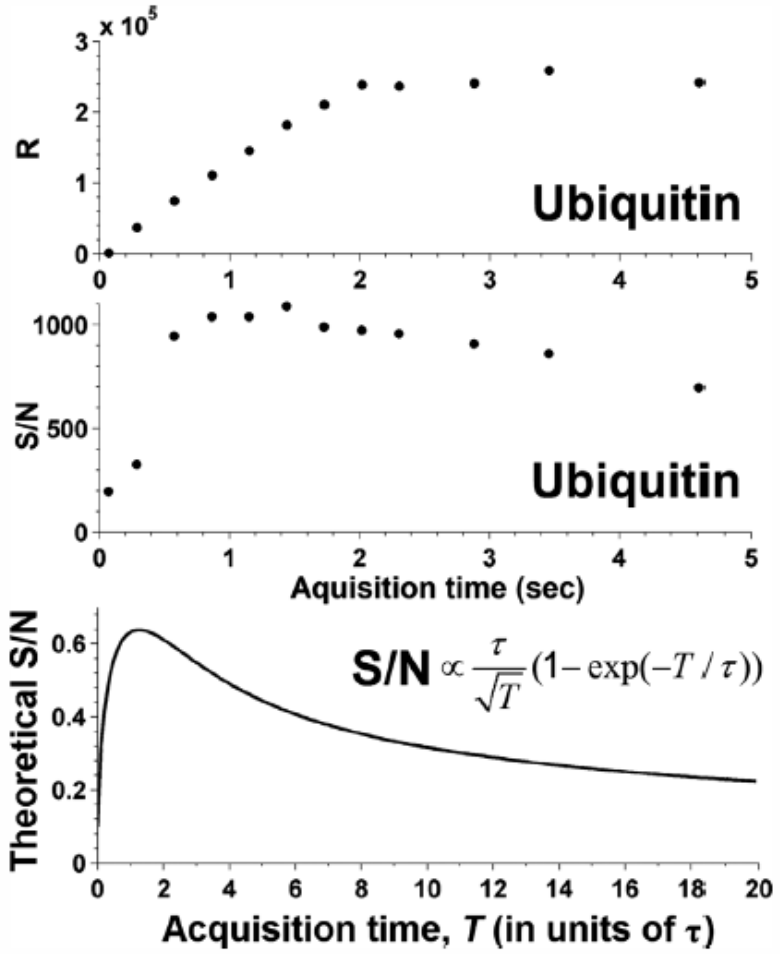

FIGURE 7. Top and middle: Plot of the transient acquisition time versus mass resolving power and S/N for the peak labeled in Figure 5 for the ubiquitin spectra. Bottom: Relative S/N of a single transient as a function of data acquisition time, *T*, at a fixed damping factor, τ.

Qi, Y.; O'Connor, P. B., Data processing in Fourier transform ion cyclotron resonance mass spectrometry. *Mass Spectrometry Reviews* ***2014, 33 (5), 333-352.***

Resolving Power in FTMS

Many other factors influence resolving power:

1. Pressure in the analyzer cell:

   Collisions with background gas destroy the coherent cyclotron motion of the ions.

2. Magnetic field inhomogeneity:

   The ion packet is dephased when the magnetic field is not uniform.

3. Space-Charge Effects:

   Ion-Ion interactions can change the ion trajectories and lead to many strange effects, like peak coalescence.

Resolving Power in FTMS

4. Excitation RF Voltage

   To achieve optimal resolving power, it is sometimes necessary to adjust the amplitude of the excitation RF voltage.

5. Data processing

   Zero filling provides more data points across a peak and improves its definition.

   Windowing removes the Gibbs oscillations and broadens the peak.

Outline

- FTICR instruments
- Pulse sequences
- Ion motion
- Equations and calibration
- Excite/detect
- Resolving power
- Space Charge
- 2-Dimensional mass spectrometry

What is “space charge”

For two charges:

$$\mathbf{F} = \frac{1}{4\pi\varepsilon_0}\frac{q_1 q_2(\mathbf{r}_1 - \mathbf{r}_2)}{|\mathbf{r}_1 - \mathbf{r}_2|^3} = \frac{1}{4\pi\varepsilon_0}\frac{q_1 q_2}{r^2}\hat{\mathbf{r}}_{21},$$

For many charges:

$$\mathbf{F}(\mathbf{r}) = \frac{q}{4\pi\varepsilon_0}\sum_{i=1}^{N}\frac{q_i(\mathbf{r} - \mathbf{r}_i)}{|\mathbf{r} - \mathbf{r}_i|^3} = \frac{q}{4\pi\varepsilon_0}\sum_{i=1}^{N}\frac{q_i}{R_i^2}\hat{\mathbf{R}}_i,$$

http://en.wikipedia.org/wiki/Coulomb’s_law

First: Global frequency shifts

$$\omega_{\text{obs}} = \frac{qB}{m} - \frac{2aV}{a^2 B} - \frac{q\rho G_i}{\epsilon_o B}$$

With this linear correction term, +/- 5 ppm mass accuracy was routinely achieved

Often this linear correction is insufficient due to the inability to account for low intensity ‘chemical noise’ ions

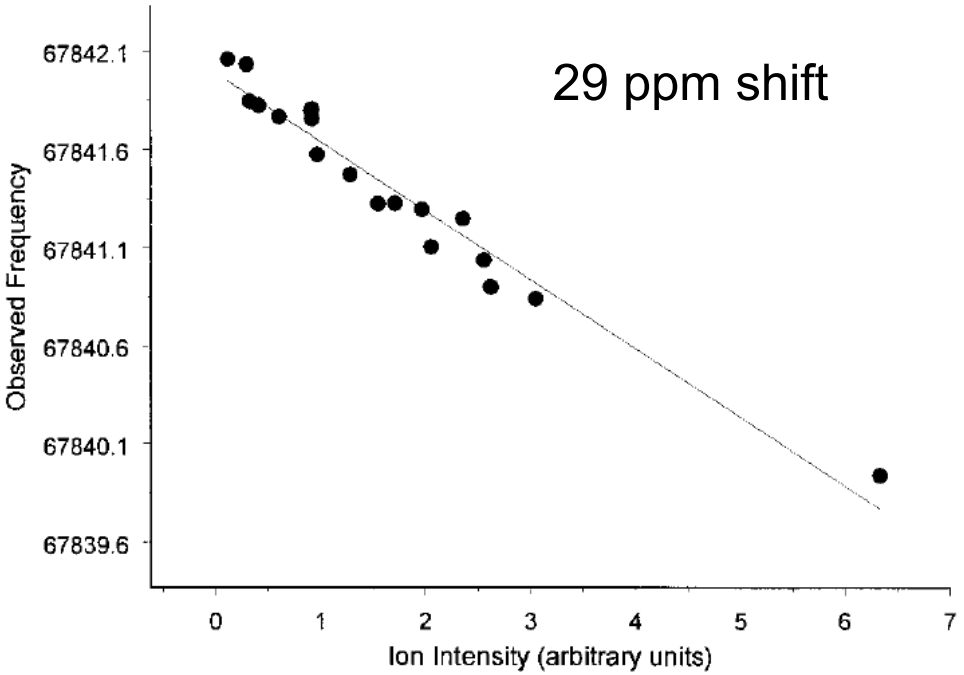

Figure 1. Frequency shift as a function of ion population for the monoisotopic peak of bradykinin, showing the change in observed frequency as a function of total ion intensity as ions from a single laser shot are remeasured.

T. J. Francl, M. G. Sherman, R. L. Hunter, M. H. Locke, W. D. Bowers, R. T. McIver, *Int. J. Mass Spec.* 1983, *54*. 189-199.
M. L. Easterling, T. H. Mize, I. J. Amster, *Anal. Chem.* 1999, *71*. 624-632.

Second: Local frequency shifts

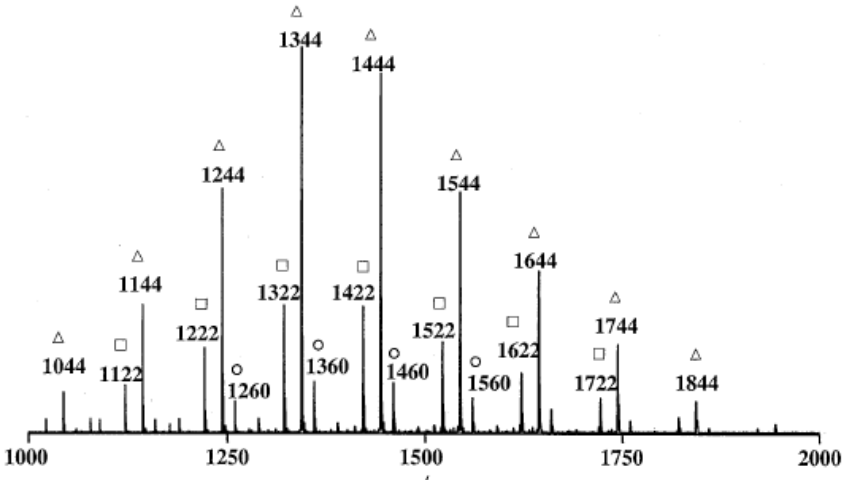

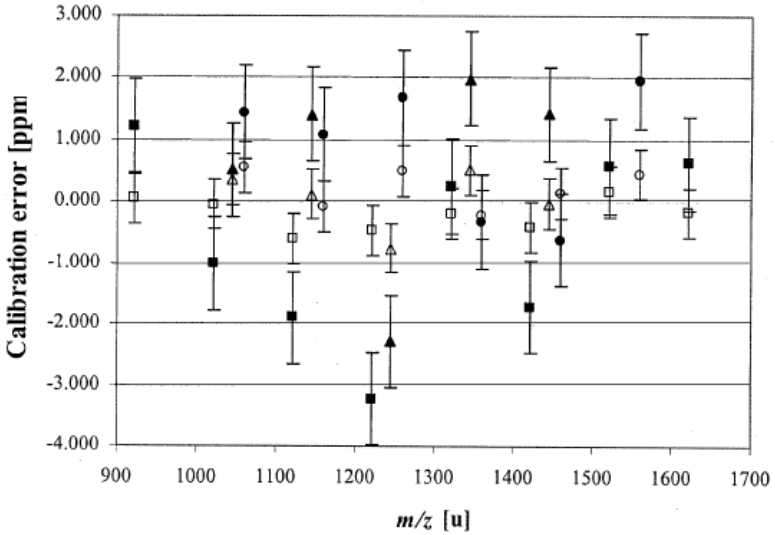

Figure 3. Calibration errors obtained from the linear fit from Eq (2) versus *m/z* for external accumulation times 400 ms (open symbols) and 600 ms (filled symbols) using chirp excitation (symbols as in Figure 2). Error bars represent 95% confidence intervals based on 10 measurements.

See also recent results by RD Smith group and DC Muddiman groups on multiple linear regression and neural network approaches toward solving this problem.

C. Masselon, A. V. Tolmachev, G. A. Anderson, R. Harkewicz, R. D. Smith, *J. Am. Soc. Mass Spectrom.* 2002, *13*. 99-106.

Third/fourth: Peak Coalescence

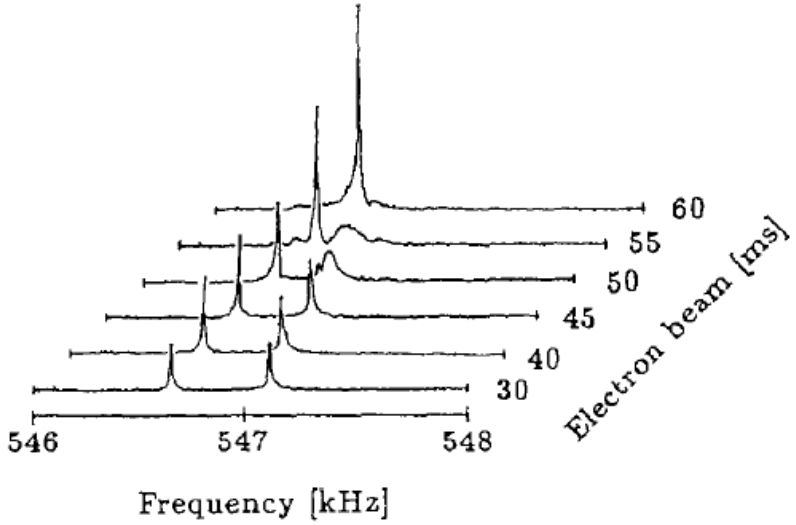

Fig. 1. Experimental results of CO^+ and $C_2H_4^+$ spectra on varying the electron beam irradiation time. The spectra were obtained using our laboratory-built FT-ICR mass spectrometer, with the magnetic field set at 0.998 T. The background pressure in the vacuum chamber was kept below 1×10^{-8} Torr. Equal amounts of CO and C_2H_4 samples were introduced through a variable leak valve and the total pressure was kept at 4.6×10^{-8} Torr. The gas was ionized by a 70 eV pulsed electron beam.

Y. Naito, M. Inoue, *Int. J. Mass Spectrom. Ion Processes* 1996, *157*. 85-96.

Third/fourth: Peak shape distortion

As the space charge causes expansion of the ion cloud, the net space charge term decreases in magnitude, so the frequency increases, causing a frequency shift.

The shift is not usually as smooth and predictable as shown here.

Most of the frequency shift occurs at the beginning of the transient.

Apodization “smooths out” this frequency shift, so that you can’t tell if/when it is occurring.

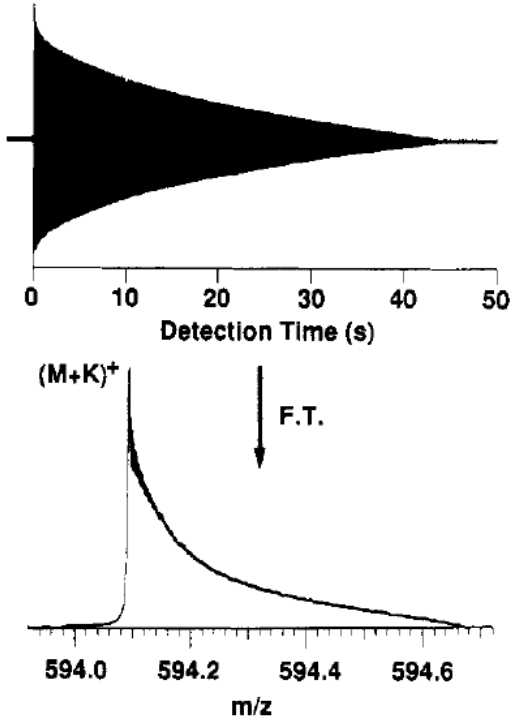

Figure 2. Time-domain ion cyclotron resonance signal (top) and magnitude-mode Fourier transform mass spectrum (bottom) of pseudomolecular ions, $(M + K)^+$, of leucine enkephalin, transferred to and detected in the analyzer trap after quadrupole excitation/collisional cooling to axialize the ions in the source trap.

S. Guan, M. C. Wahl, A. G. Marshall, *Anal. Chem.* 1993, *65*. 3647-3653.

Third/fourth: Peak shape distortion – extreme case

SLCC eliminates signal coherence in, typically, 10's of milliseconds.

SLCC or "nipple" occurs at the point where magnetron expansion (from space charge) causes the magnetron radius to equal the cyclotron radius.

At this point, the ion packets experience high velocity "coulombic" collisions at the center of the cell – causing scattering and rapid dephasing of the ion cloud.

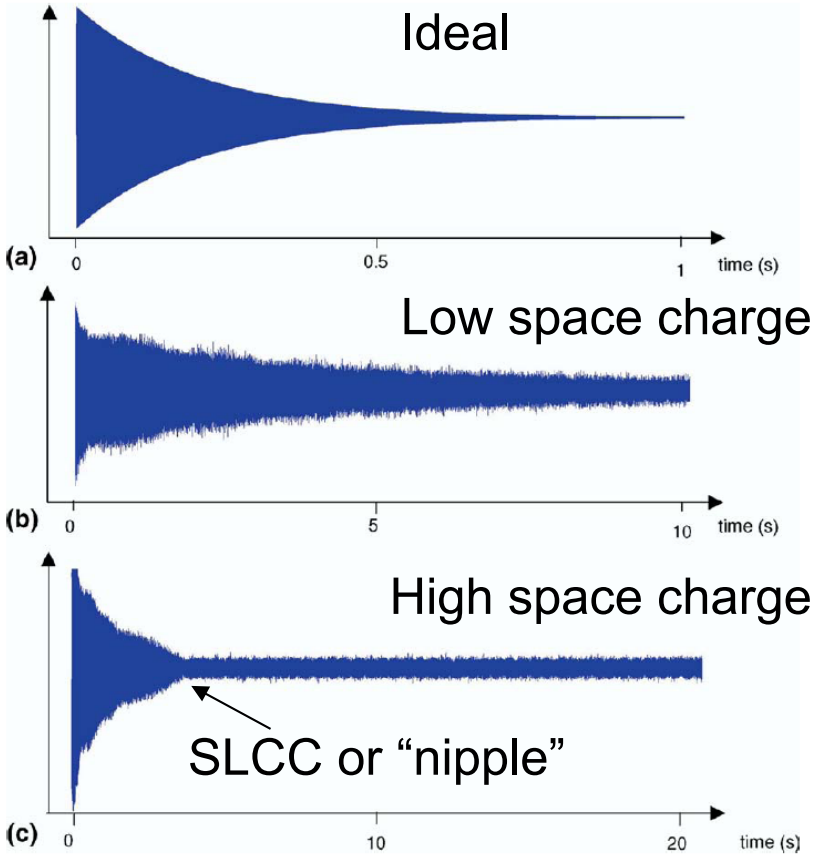

Figure 1. Examples of the transient signals: (a) hypothetical exponentially decaying sinusoidal signal; (b) transient of a high-resolution substance-P spectrum; (c) an example of SLCC where a period of exponential decay is followed by a rapid noncorrelated decay.

K. Aizikov, R. Mathur, P. B. O'Connor, The Spontaneous Loss of Coherence Catastrophe in Fourier Transform Ion Cyclotron Resonance Mass Spectrometry. *J. Am. Soc. Mass Spectrom.* 2009, *20*. 247-256.

Fifth: Resolution decrease

If frequencies are shifting (due to space charge), the ion packet is dephasing – shortening the transient.

Shorter transients result in lower resolution.

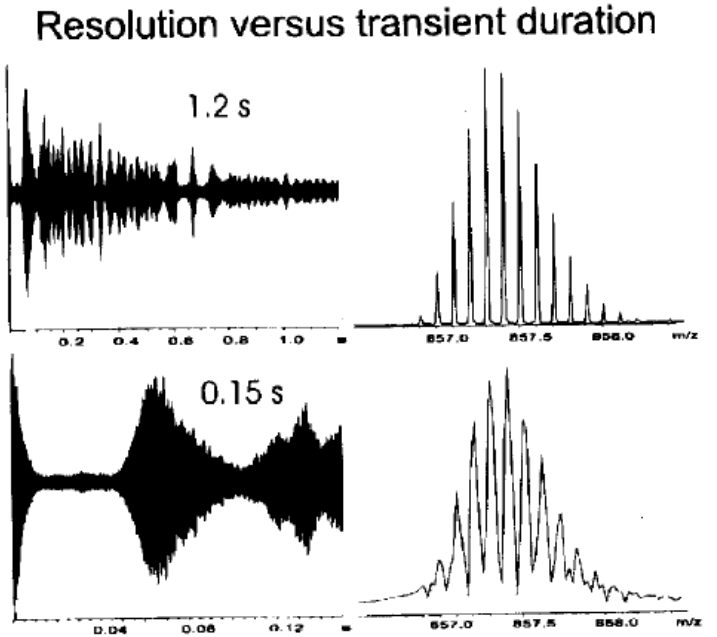

Figure 10. An illustration of the relationship between the length of the transient that is examined and the resolution that can be achieved. The top mass spectrum is obtained from a 1.2 s transient and exhibits a resolution of ~90 000 (FWHM). The bottom mass spectrum is obtained from the first eighth of the same transient (150 ms) and exhibits eight times lower resolution, ~12 000 (FWHM).

I. J. Amster, Fourier Transform Mass Spectrometry. *J. Mass Spectrom.* 1996, *31*. 1325-1337.

Achieving High Mass Resolution

- Acquire long transients (RP = fT/2)
- Use low trapping potentials (less than 1 V)
- Carefully control space charge
- Maintain ultrahigh vacuum (P = 10^{-9} torr or lower)
- Tune excitation amplitude
- Ion gymnastics (e.g. QE) may be necessary

Outline

- FTICR instruments
- Pulse sequences
- Ion motion
- Equations and calibration
- Excite/detect
- Resolving power
- Space Charge
- 2-Dimensional mass spectrometry

Original Ion Excitation/De-excitation Experiment

Coherently excited ions in ICR cell:

- Excitation voltage ***in phase with*** ion motion: ions excited to higher radius
- Excitation voltage ***in phase opposition with*** ion motion: ions de-excited to center of ICR cell.

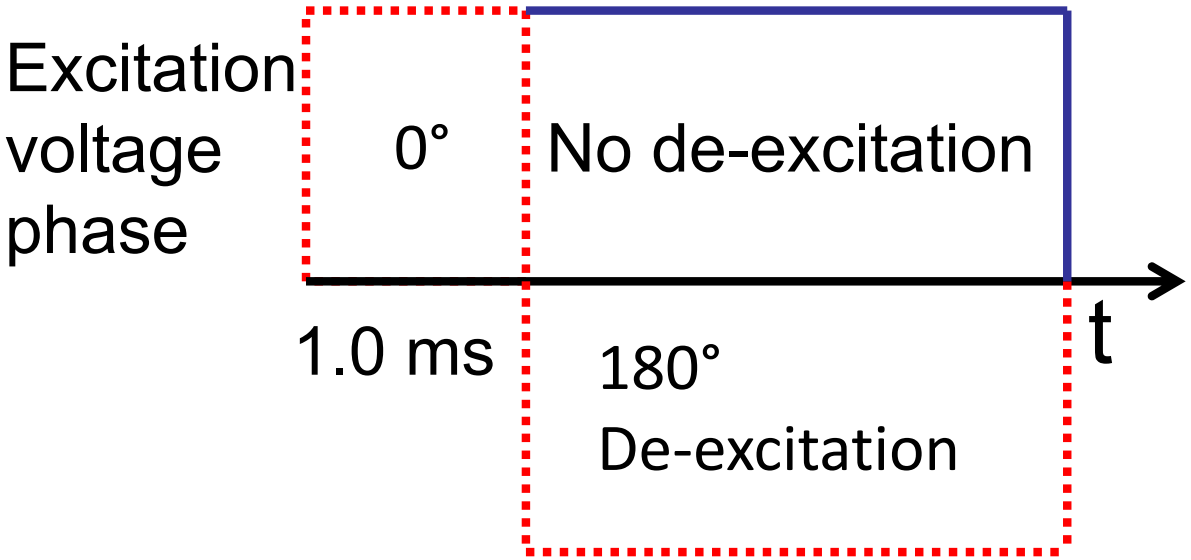

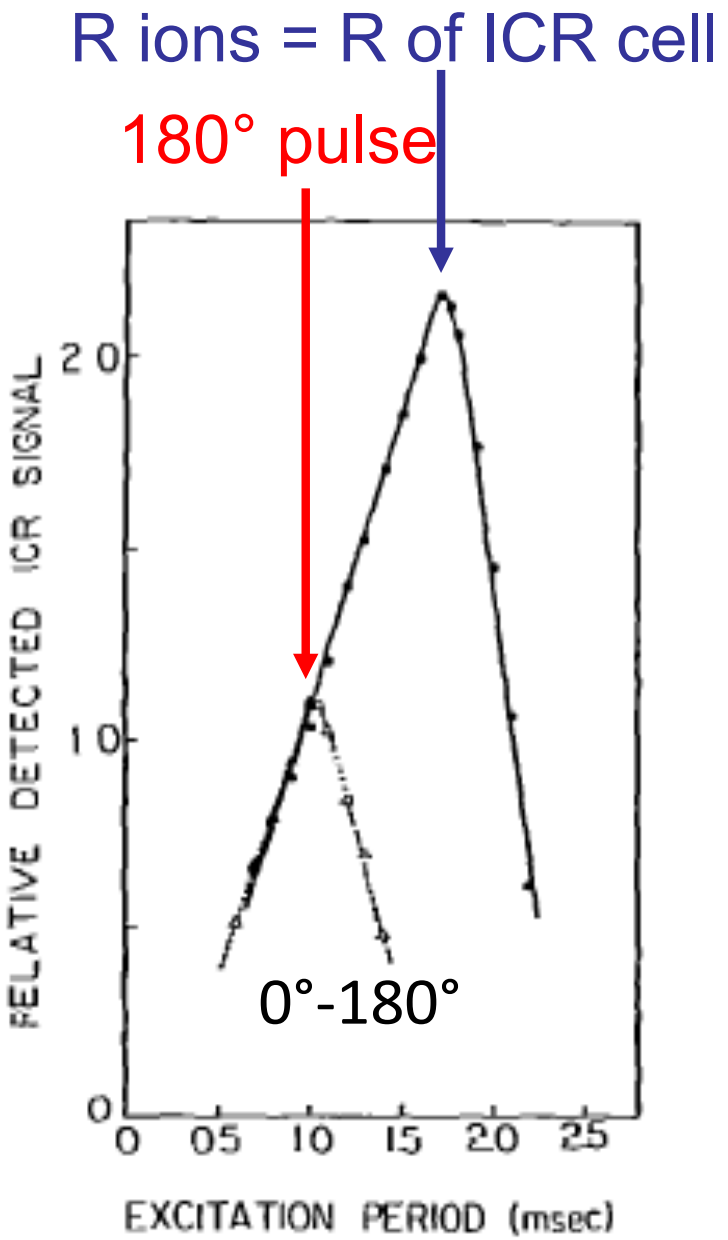

A.G. Marshall, T.C. Lin Wang, T. Lebatuan Ricca, *Chem. Phys. Letts.* 105 (1984) 233-236.

2D FTICR-MS

- All ions in a complex sample fragmented and visualised on one spectrum

- NO isolation
- YES fragmentation

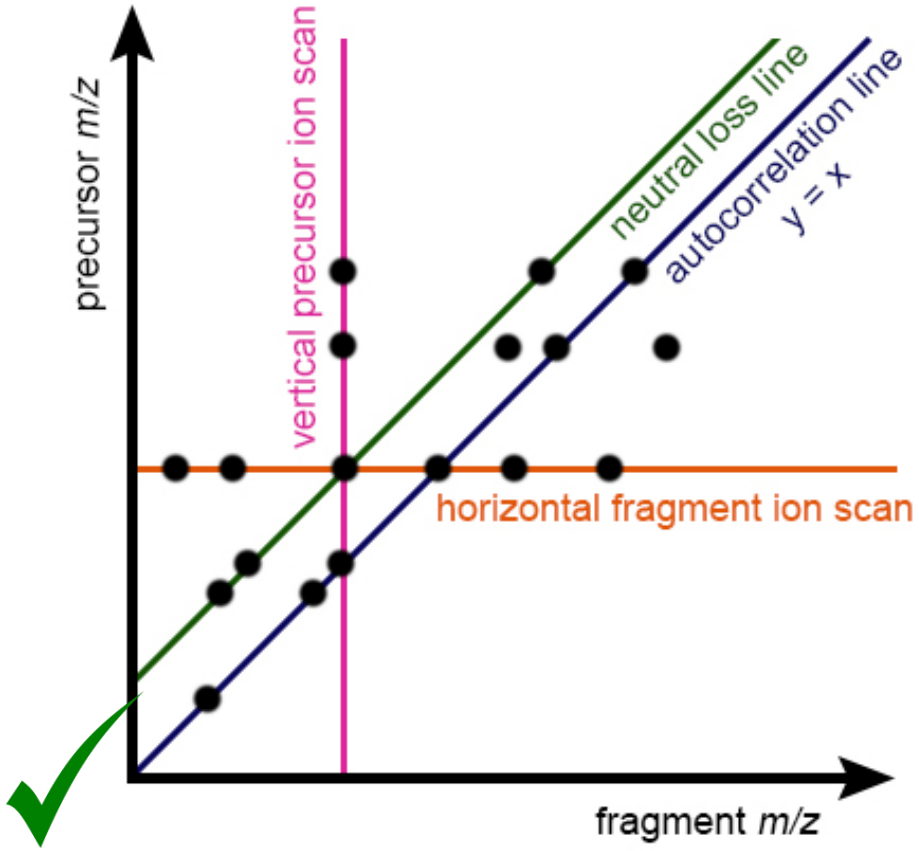

M. A. van Agthoven, M.-A. Delsuc, G. Bodenhausen and C. Rolando, *Analytical and Bioanalytical Chemistry*, 2013, **405**, 51-61.

Raw 2D-FTICR-MS of Yeast Tryptic Digest (8th July, 2015)

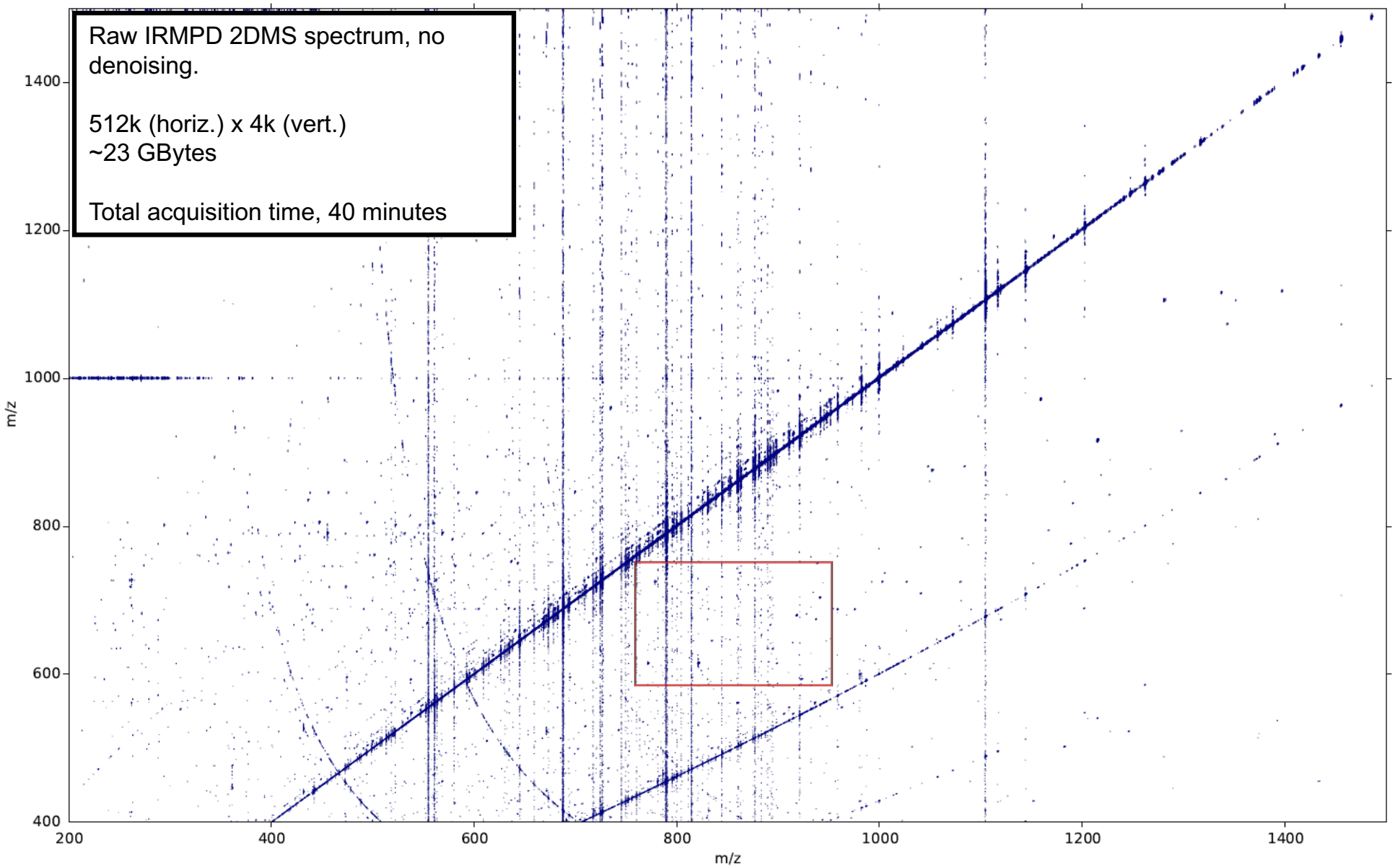

2DMS of Yeast tryptic digest, expansion of the ~600-700 Da (precursor ion) and ~750-950 Da (product ion) region.

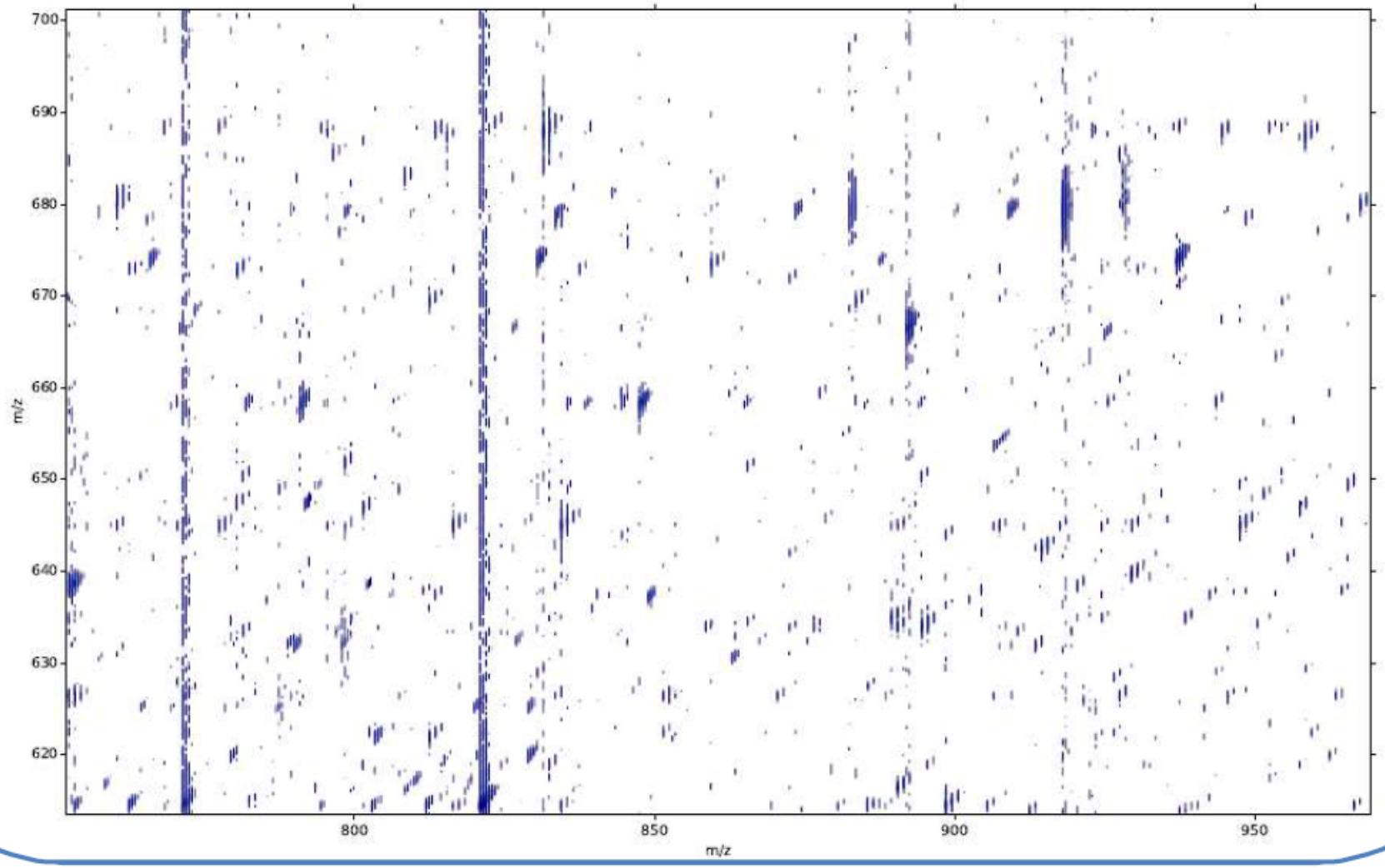

Acknowledgements

People
Dr. Huilin Li, Dr. Yulin Qi, Cookson Chiu, Dr. Andrea Lopez-Clavijo, Dr. Pilar Perez-Hurtado, Meng Li, Samantha Benson, Dr. Rebecca Wills, Dr. Mark Barrow, Matthew Griffiths, Dr. Ron Heeren, Dr. Haytham Hussein, David Kilgour, Dr. Terry Lin, Andrew Soulby, Dr. Juan Wei, Chris Wootton, Hayley Simon, Dr. Maria van Agthoven, Federico Floris, Dr. Parminder Kaur, Dr. Raman Mathur, Dr. Jason Cournoyer, Dr. Nadia Sargaeva, Dr. Xiaojuan Li, Dr. MD. Jason Pittman, Dr. Bogdan Budnik, Dr. Susanne Moyer, Dr. Vera Ivelva, Dr. Konstantine Aizikov, Haytham Hussein, Mark Kozlowski, Samuel Peel, Yuko (Pui Yiu) Lam, Holly Chan, Man Ying Wong.

- Warwick Postgraduate Research Scholarship (WPRS)
- Department of Chemistry, University of Warwick
- Warwick Centre for Analytical Science
- Warwick Impact Fund
- Bruker
- NIH
- ERC
- EPSRC (J003022/1, N021630/1)

EPSRC
Engineering and Physical Sciences Research Council